# Immune checkpoint inhibitors reverse tolerogenic mechanisms induced by melanoma targeted radionuclide therapy

Jacques Rouanet, Valentin Benboubker, Hussein Akil, Ana Hennino, Philippe Auzeloux, Sophie Besse, Bruno Pereira, Solène Delorme, Sandrine Mansard, Michel d'Incan, et al.

Cancer Immunology, Immunotherapy (2020) 69:2075–2088
https://doi.org/10.1007/s00262-020-02606-8

ORIGINAL ARTICLE

# Immune checkpoint inhibitors reverse tolerogenic mechanisms induced by melanoma targeted radionuclide therapy

**Jacques Rouanet[1,2,3] · Valentin Benboubker[1,4] · Hussein Akil[1] · Ana Hennino[5] · Philippe Auzeloux[1] · Sophie Besse[1] · Bruno Pereira[6] · Solène Delorme[1] · Sandrine Mansard[2] · Michel D'Incan[1,2] · Françoise Degoul[1] · Paul-Olivier Rouzaire[1,4]**

Received: 3 February 2020 / Accepted: 12 May 2020 / Published online: 23 May 2020


## Abstract

In line with the ongoing phase I trial (NCT03784625) dedicated to melanoma targeted radionuclide therapy (TRT), we explore the interplay between immune system and the melanin ligand [$^{131}$I]ICF01012 alone or combined with immunotherapy (immune checkpoint inhibitors, ICI) in preclinical models. Here we demonstrate that [$^{131}$I]ICF01012 induces immunogenic cell death, characterized by a significant increase in cell surface-exposed annexin A1 and calreticulin. Additionally, [$^{131}$I]ICF01012 increases survival in immunocompetent mice, compared to immunocompromised (29 vs. 24 days, $p = 0.0374$). Flow cytometry and RT-qPCR analyses highlight that [$^{131}$I]ICF01012 induces adaptive and innate immune cell recruitment in the tumor microenvironment. [$^{131}$I]ICF01012 combination with ICIs (anti-CTLA-4, anti-PD-1, anti-PD-L1) has shown that tolerance is a main immune escape mechanism, whereas exhaustion is not present after TRT. Furthermore, [$^{131}$I]ICF01012 and ICI combination has systematically resulted in a prolonged survival ($p < 0.0001$) compared to TRT alone. Specifically, [$^{131}$I]ICF01012 + anti-CTLA-4 combination significantly increases survival compared to anti-CTLA-4 alone (41 vs. 26 days; $p = 0.0011$), without toxicity. This work represents the first global characterization of TRT-induced modifications of the antitumor immune response, demonstrating that tolerance is a main immune escape mechanism and that combining TRT and ICI is promising.

**Keywords** Targeted radionuclide therapy · Metastatic melanoma · Immune checkpoint inhibitor · Tolerance · Melanin · Anti-βig-h3

## Abbreviations

| | |
|---|---|
| Ab | Antibody |
| DAMPs | Damage-associated molecular pattern molecules |
| EBRT | External beam radiation therapy |
| ICI | Immune checkpoint inhibitors |
| NK | Natural killer |
| TRT | Targeted radionuclide therapy |

Françoise Degoul and Paul-Olivier Rouzaire have contributed equally to this work.

**Electronic supplementary material** The online version of this article (https://doi.org/10.1007/s00262-020-02606-8) contains supplementary material, which is available to authorized users.

✉ Jacques Rouanet
jacques.rouanet@inserm.fr

[1] UMR1240 INSERM, Université Clermont Auvergne, 58, rue Montalembert, BP 184, 63005 Clermont-Ferrand, France

[2] Department of Dermatology and Oncodermatology, CHU Estaing, 1 place Lucie et Raymond Aubrac, 63000 Clermont-Ferrand, France

[3] Centre Jean Perrin, 58, rue Montalembert, 63011 Clermont-Ferrand, France

[4] Department of Histocompatibility and Immunogenetics, CHU Gabriel Montpied, 58 rue Montalembert, 63000 Clermont-Ferrand, France

[5] UMR INSERM 1052 CNRS 5286 CRCL, 28 rue Laennec, 69008 Lyon, France

[6] Biostatistics Unit, DRCI, CHU Gabriel Montpied, 58 rue Montalembert, 63000 Clermont-Ferrand, France

## Introduction

Cutaneous melanoma is one of the deadliest types of skin cancer, developing from epidermis melanocytes—cells specialized in melanin synthesis. Since 2010, the emergence of new specific treatments has heavily modified metastatic melanoma prognosis, especially MAPK-targeted therapies and immunotherapy. Melanoma is an obvious candidate for immunotherapy due to its high mutational burden [1], leading to a high number of potential neoantigens. However, stimulating immune response is a challenge since melanoma cells develop mechanisms to avoid or annihilate it. These immune escape mechanisms involve (1) decrease in antigen expression, CMH molecules or natural killer (NK) cell co-activator ligands, (2) inhibition of co-stimulatory signals, (3) expression of co-inhibitors, (4) induction of T cell exhaustion and (5) tolerogenic immune response [2]. Classical oncologic treatments (such as external beam radiation therapy, EBRT [3]) can boost these mechanisms. On the other hand, a strategy of immunotherapy consists in reversing these immune escape mechanisms using immune checkpoint inhibitors [4] (i.e., anti-CTLA-4 and anti-PD-1 antibodies, Abs). CTLA-4 and PD-1 are immune checkpoint receptors that downregulate T cell activation involved in immunologic tolerance. CTLA-4 is expressed by T regulatory cells and upregulated in activated T cells. CTLA-4 is a CD28 homologue that competes with CD28 to interact with B7 ligands to inactivate T cells [5]. PD-1 is expressed by activated T cells, monocytes, B cells and NK cells. PD-1 interaction with its ligands, PD-L1 or PD-L2, inhibits T cell receptor signaling and prevents T cell activation as well as proinflammatory cytokine secretion [6]. PD-1 is the main marker of T cell exhaustion. Therapeutic inhibition of PD-1 and of CTLA-4 in melanoma induces persistent response and long-term survival [4]. Other immune checkpoint inhibitors (ICIs) are currently being tested in clinical trials (for instance, Ab against Lag3) [4]. Another interesting approach consists in depleting βig-h3, a matrix protein expressed upon TGF-β signaling, with a specific Ab. βig-h3 is highly expressed in melanoma and associated with bad prognosis and metastatic spread [7]. βig-h3 via interactions with integrin β3 inhibits proliferation and activation of $CD8^+$ cells and macrophages in tumor microenvironment. Therefore, a βig-h3-depleting mAb significantly decreased tumor growth by promoting antitumor immunity in a murine model of pancreatic ductal adenocarcinoma [8, 9].

The impact of EBRT on the immune response involves both innate and adaptive mechanisms [3], and EBRT has been successfully used in combination with ICIs in both preclinical models [10] and clinical trials [11, 12]. Ionizing radiations enhance antitumor immune response by releasing antigens and inducing neoantigens expression, by increasing expression of co-stimulatory or co-inhibitory molecules or CMH molecules, by recruiting immune cells in the tumor microenvironment such as $CD8^+$ T cells and regulatory T cells and by provoking immunogenic death. Immunogenic death [13] is a form of cell death induced by irradiation as well as chemotherapy, which leads to expression of damage-associated molecular pattern molecules (DAMPs) by the tumor cells. These DAMPs are immunostimulatory signals that activate antigen-presenting cells and promote cytotoxic T cell response. DAMP signals consist in the externalization of calreticulin and annexin A1 [14], in the release of HMGB1 and ATP in the extracellular matrix and in the secretion of IFN-1.

Few data are available regarding consequences of targeted radionuclide therapy (TRT) on antitumor immune response. A study has shown that TRT using $^{177}$Lu-DOTA-TATE induces recruitment of CD86-bearing antigen-presenting cells and NK cells in murine neuroendocrine tumor microenvironment [15]. Additionally, the use of $^{224}$Ra wires in different tumor models induces an immune T response [16]. Combination of a $^{90}$Y radiolabeled anti-CEA mAb with an antitumoral vaccine induces a $CD4^+$ and $CD8^+$ T-response in a murine carcinoma model [17]. Recently, Hernandez et al. have demonstrated that a $^{90}$Y radiolabeled alkylphosphocholine (NM600) induces a memory T cell response in a lymphoma syngeneic model [18].

Thus, combining TRT with ICIs might be of major interest since it could increase ICIs efficacy. Recently, Choi et al. have combined ICI with a TRT approach using a $^{177}$Lu-radiolabeled peptidomimetic targeting very late antigen-4 (VLA-4) [19], an integrin highly expressed in melanoma as well as in immune cells. In this preclinical study, TRT combined with dual ICI (anti-CTLA-4 + either anti-PD-1 or anti-PD-L1) has led to a benefit in median survival (22 days and 23 days, respectively) compared to TRT alone (19 days).

Our group has developed [$^{131}$I]ICF01012, a radiolabeled melanin ligand for metastatic melanoma TRT [20], which specifically binds to pigmented melanoma [21]. In murine syngeneic [22] and xenograft [23] preclinical models, systemic injection of [$^{131}$I]ICF01012 reduces tumor growth and extends survival time, with minimal toxicity [24]. A phase I clinical trial of [$^{131}$I]ICF01012 is currently ongoing in order to evaluate its toxicity and assess the appropriate therapeutic dose in human (NCT03784625). Here we study the interaction between immune system and [$^{131}$I]ICF01012 TRT using functional and molecular in vitro and in vivo approaches in the murine B16F10 model. We also evaluate the efficacy of combined use of [$^{131}$I]ICF01012 with different ICI (anti-CTLA4, anti-PD1 and anti-PDL1) and with an anti-βig-h3 Ab.

## Materials and methods

### Cell culture and cell lines

Murine B16F10 melanoma cell line was purchased from the ATCC in 2005 and grown as previously described [25]. Cells were free of mycobacterial contamination tested by PCR (EUROFINS) in 10/2018.

### Murine models

Experimentations on mice were in conformity with the Guide for the Care and Use of Laboratory Animals published by the US National Institutes of Health (8th edition, 2011) and were approved by local Ethic committee of Clermont-Ferrand (C2E2A no. 002) and French Ministry of Education and Research (Approval No. 12211-2017111613576925). B16F10 cells ($2\times10^5$) were injected subcutaneously in the right flank of 5-week-old female mice. C57BL6/J wild-type mice were purchased at Charles River (L'Arbresle, France), and *Rag2*$^{KO}$ mice were provided by Dr Hennino (INSERM U1052, Lyon, France).

### Therapy protocols

[$^{131}$I]ICF01012 was prepared according to Chezal et al. [20].

*[$^{131}$I]ICF01012 monotherapy* B16F10(C57BL/6 J) and B16F10(*Rag2*$^{KO}$) mice were injected intravenously with either 18.5 MBq/100 µL of [$^{131}$I]ICF01012 or with 100 µL of vehicle ten days after tumor implantation.

*Combinations* B16F10(C57BL/6 J) mice received four intraperitoneal injections of immunotherapy or corresponding isotype (Supplementary Table 3) days 6, 10, 14 and 18 post-tumor implantation. Anti-PD-1, anti-PD-L1 and anti-CTLA-4 antibodies were purchased at BioXCell (Lebanon, USA) and used at the dose of 200 µg per injection. Anti-βig-h3 antibody was provided by Dr HENNINO and used at the dose of 6 µg per injection. After the second antibody injection, mice were injected intravenously with [$^{131}$I]ICF01012 (18.5 MBq/100 µL) or vehicle (100 µL).

### Follow-up and survival study

Body weight and tumor volume were measured three times a week until tumor volume reached 1000 mm$^3$ and then daily. Tumor volume was calculated from the measurement of two perpendicular diameters using a caliper according to the formula $L\times S^2/2$, where L and S are the largest and smallest diameters, respectively, expressed in millimeters. Mice were killed when tumor volume reached approximately 2000 mm$^3$ or in case of a weight loss reaching 20% or at experiment time. Adverse events were monitored daily. Doubling times (DT) have been calculated individually for each animal as previously described [22].

### Tumor collection

B16F10(C57BL/6J) mice were killed at day ten post-intravenously injection of [$^{131}$I]ICF01012 for immunofluorescence and RTqPCR analyses and at day 3, day 6 and day 12 post-i.v. injection of [$^{131}$I]ICF01012 for flow cytometry analyses. For TLDA analysis, B16F10(C57BL/6 J) mice were harvested when they reached the survival endpoint. Tumors were frozen in liquid nitrogen and stored at − 80 °C for RT-qpCR and TLDA analysis, or fixed in 10% neutral buffered formalin (Sigma) and stored in 70% ethanol for immunofluorescence analysis. Flow cytometry analyses were performed on fresh tumor in RPMI 1640 (Invitrogen).

### Immunofluorescence

Immunofluorescence was performed as previously described [25]. The following primary Abs were used: rabbit polyclonal anti-annexin A1 (1/200, ThermoFischer® #71-3400) and recombinant rabbit monoclonal anti-calreticulin (1/500, Abcam ab92516). Isotype controls used irrelevant normal rabbit IgG (Sigma). Slides were then incubated with fluorescence-conjugated secondary Ab to rabbit IgG (1/500; Invitrogen) for 1 h at RT. Nuclei were stained with DAPI (0.1 µg/mL; Sigma). After slide mounting with Vectashield, emitting fluorescence was detected using SPE confocal microscope (Leica) and analyzed with Fiji software.

### Flow cytometry

Antibodies (Supplementary Table 4) for flow cytometry were provided by BD Biosciences®. Tumors were totally dissociated with a tumor dissociation kit mouse (Miltenyi Biotec®). After filtration and wash, cells were incubated in staining buffer with a mixture of the anti-mouse-conjugated antibodies for 15 min in the dark at 4 °C. Gating was performed among CD45 + cells. NK cells were identified as CD3$^-$/NKp46$^+$, CD8$^+$ T cells were identified as CD45$^+$/CD3$^+$/CD8$^+$ cells, CD4$^+$ T cells were identified as CD45$^+$/CD3$^+$/CD4$^+$ cells, and regulatory T cells were identified as CD45$^+$/CD4$^+$/CD127$^{low}$ cells. Absolute quantification was obtained using CountBright beads (Invitrogen).

### RT-qPCR

Extraction of RNA was performed on 30 mg of tumor with RNA Extraction Kit (Macherey–Nagel, Hoerdt, France). To represent tumor heterogeneity, two distant samples from each tumor (4 controls, 5 TRTs) were used. cDNA was

synthesized from 2500 ng of RNA with SuperScript™ IV VILO™ Master Mix (ThermoFisher, Courtaboeuf, France). Two transcriptase reverse reactions were done for each sample and pooled. qPCRs (Supplementary Table 5) were realized in triplicate with SYBR® Mix (KAPABIOSYSTEMS, Boston, USA) on a StepOnePlus device (Applied BioSystems, Foster City, USA). PCR product specificity was verified with a melting curve procedure. Results were calculated with the ΔΔCT method after normalizing the expression to that of *Ubiquitin C* and *GAPDH*.

### Transcriptomic analyses

Extraction of whole-tumor RNA and reverse transcription were realized using the above protocol. Pre-designed TaqMan probe and primer sets for 64 target genes were chosen from an online catalogue (Applied Biosystems). Gene families were immune response ($n=40$), epithelial–mesenchymal transition ($n=20$) and stemcellness ($n=4$). Once selected, the sets were factory loaded into the 384 wells of TaqMan low-density arrays (TLDAs). qPCRs were realized with a TaqMan™ Fast Advanced Master Mix (Applied Biosystems). Samples were run and analyzed using the 7900HT system with a TLDA Upgrade (Applied Biosystems) according to the manufacturer's instructions. Gene expression values were calculated with the ΔΔCT method after normalizing the expression to that of *Gapdh*, *TPB* and *Ubiquitin c*. For each gene, expression in TRT + anti-CTLA-4, TRT + anti-CTLA-4 + anti-PD-1 and TRT + anti-CTLA-4 + anti-PD-L1 tumors was compared to that of TRT alone treated tumors.

### Statistics

Statistical analyses were conducted using Stata software (StataCorp, College Station, Texas, USA) and Prism software (GraphPad, San Diego, California, USA). A two-tailed *p* value of less than 0.05 was considered to indicate statistical significance.

For RT-qPCR analysis, the fold changes (Control *vs* TRT) are expressed as mean ± SD and were compared with Student's t test. The normality assumption was analyzed using Shapiro–Wilk's test. TLDA analyses were compared using one-way ANOVA. For the analysis of repeated measures (tumor growth), the random effects model (REM) was considered, as usually proposed, to study the following fixed effects—treatment groups, time point evaluation and their interaction group × time − taking into account between- and within-subject variability (as random effect). Censored data (survival) were estimated using the Kaplan–Meier method. The log-rank test was used in univariate analysis for two-group comparison. These analyses were completed by Cox proportional hazards model applying a Sidak's type I error correction to take into account multiple comparisons. The proportional hazard hypothesis was studied with Schoenfeld's test. Synergy analyses were performed according to Viallard et al. [26].

## Results

### TRT modulates antitumor immune response

Expression of annexin A1 and calreticulin, which are known immunogenic cell death markers, was assessed using immunofluorescence techniques. We demonstrated that [$^{131}$I] ICF01012 significantly increases annexin A1 (Fig. 1a, $p=0.0059$) and calreticulin (Fig. 1b, $p=0.0470$) expression on cell surface ten days after irradiation in a B16F10 tumor model, showing that [$^{131}$I]ICF01012 irradiation induces immunogenic cell death.

We treated *Rag2*$^{KO}$ mice to specify the involvement of the adaptive immune system in TRT efficiency. Tumor growth was significantly slower after TRT in C57BL/6 mice compared to *Rag2*$^{KO}$ mice (Fig. 1c). In the TRT-treated wild-type mice, we showed (Fig. 1d**,** Supplementary Table 1) an extension of median survival (29 days vs. 21 days, $p=0.0182$). In contrast, median survival was not different in both TRT-treated and untreated immunocompromised *Rag2*$^{KO}$ mice (Fig. 1d**,** Supplementary Table 1, 24 days vs. 21 days, $p=0.6094$). Additionally, survival was similar in both untreated groups (C57BL/6 J vs. *Rag2*$^{KO}$, 21 days vs. 21 days, $p=0.8763$). These results suggest that [$^{131}$I] ICF01012 efficacy relies on the adaptive immune system to be fully efficient.

Flow cytometry analyses revealed an initial decrease in CD45$^+$ leucocytes, CD8$^+$ T lymphocytes, CD4$^+$ T lymphocytes and NK cells three days after TRT injection (Fig. 2a); however, this decrease was non-significant. This could be related to a peripheral hematoxicity due to non-specific radiation effect of [$^{131}$I]ICF01012. However, twelve days after TRT injection, CD8$^+$ and CD4$^+$ T populations significantly increased in tumors compared to control ($p=0.0351$ and $p=0.0347$, respectively) while NK cell population increased at day 6 without reaching statistical significance (Fig. 2a). Additionally, we observed a non-significant increase in CD4$^+$ CD127$^{low}$ T regulatory cell population at day 12 in the treated tumors ($p=0.0977$).

RT-qPCR analyses (Fig. 2b) at day 10 strengthened the flow cytometry data by showing a twofold increase in the *Adgre1* (*Emr1*) and *Ncr1* (*Nkp46*) gene transcripts ($p=0.0416$ and $p=0.0285$, respectively) suggesting a

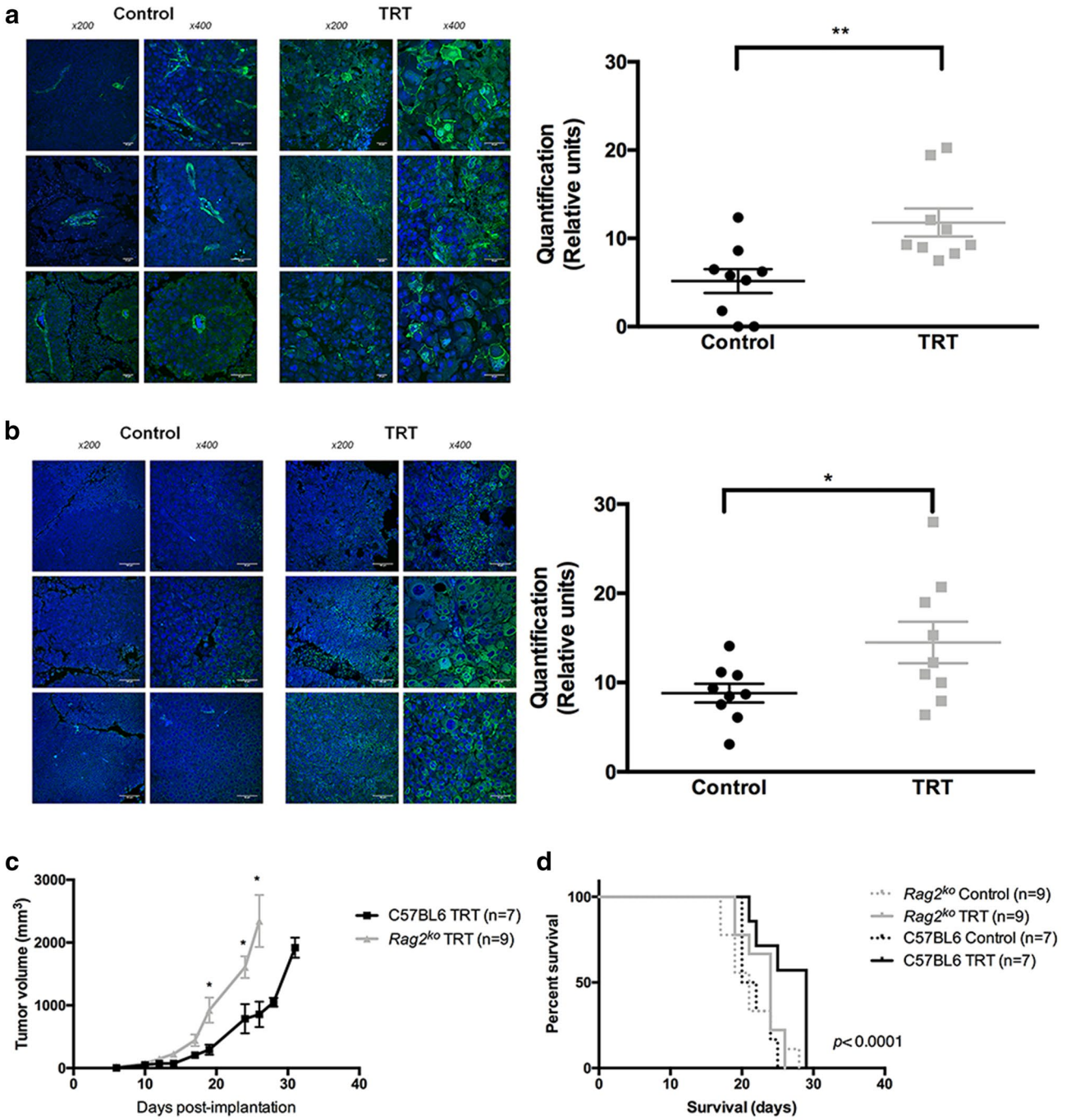


**Fig. 1** TRT induces immunogenic cell death (**a**, **b**) and depends on adaptive immune response (**c**, **d**). Cell surface expression of (**a**) annexin A1 and (**b**) calreticulin was assessed by immunofluorescence on control and treated B16F10 tumors 10 days after TRT. TRT effects on (**c**) tumor growth and (**d**) survival were compared in immunocompetent C57BL/6 J ($n=15$) and immunocompromised $Rag2^{KO}$ mice ($n=9$). (*$p<0.05$, **$p<0.01$, ***$p<0.001$, ****$p<0.0001$)

TRT-induced upregulation of the innate immune response within tumor microenvironment. Additionally, we observed expression modifications in genes related to adaptive immunity after [$^{131}$I]ICF01012 injection. Antitumor cytotoxic response genes were upregulated, with a 1.5-fold increase for *Cd8a*, *Ifnγ* and *Tnfα* ($p=0.0256$, $p=0.0456$ and $p=0.0884$, respectively) and a threefold increase for *Gzmb* ($p=0.0358$). The transcription of genes involved in immune tolerance

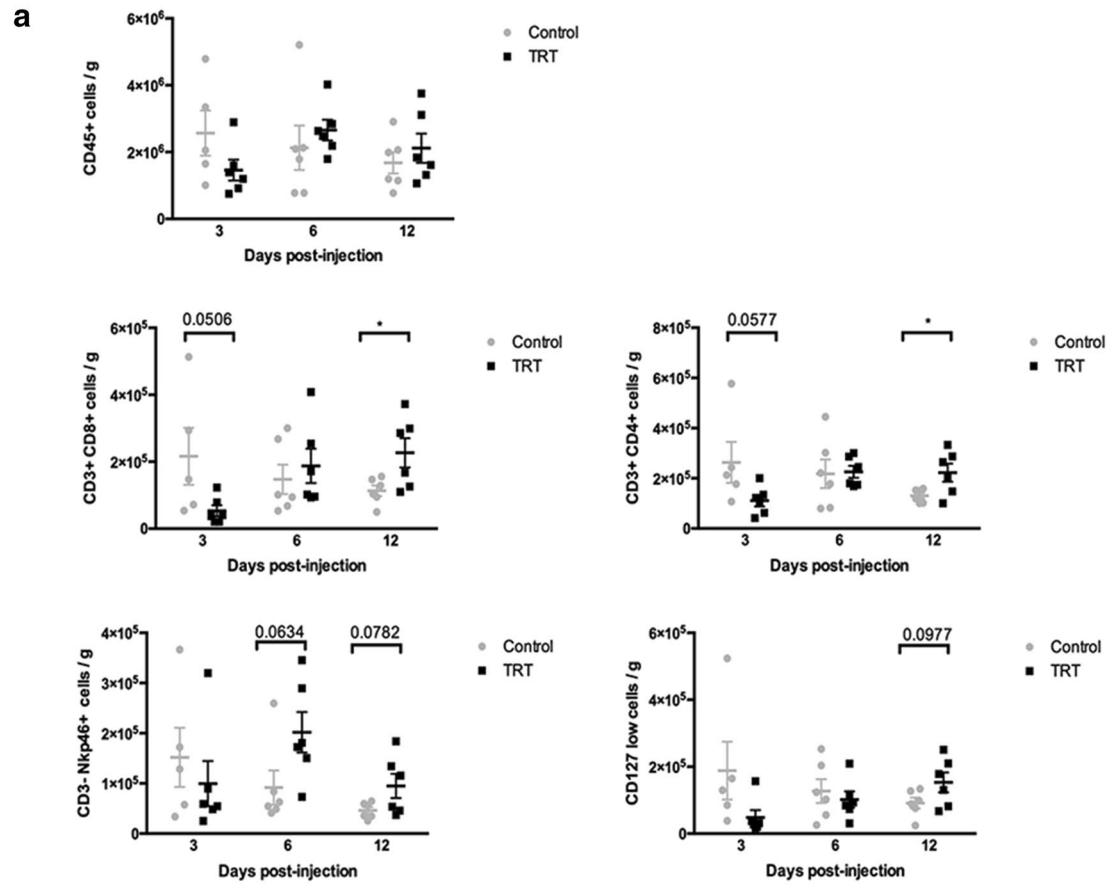
a
CD45+ cells / g
Days post-injection
Control
TRT
CD3+ CD8+ cells / g
0.0506
CD3+ CD4+ cells / g
0.0577
CD3- Nkp46+ cells / g
0.0634
0.0782
CD127 low cells / g
0.0977

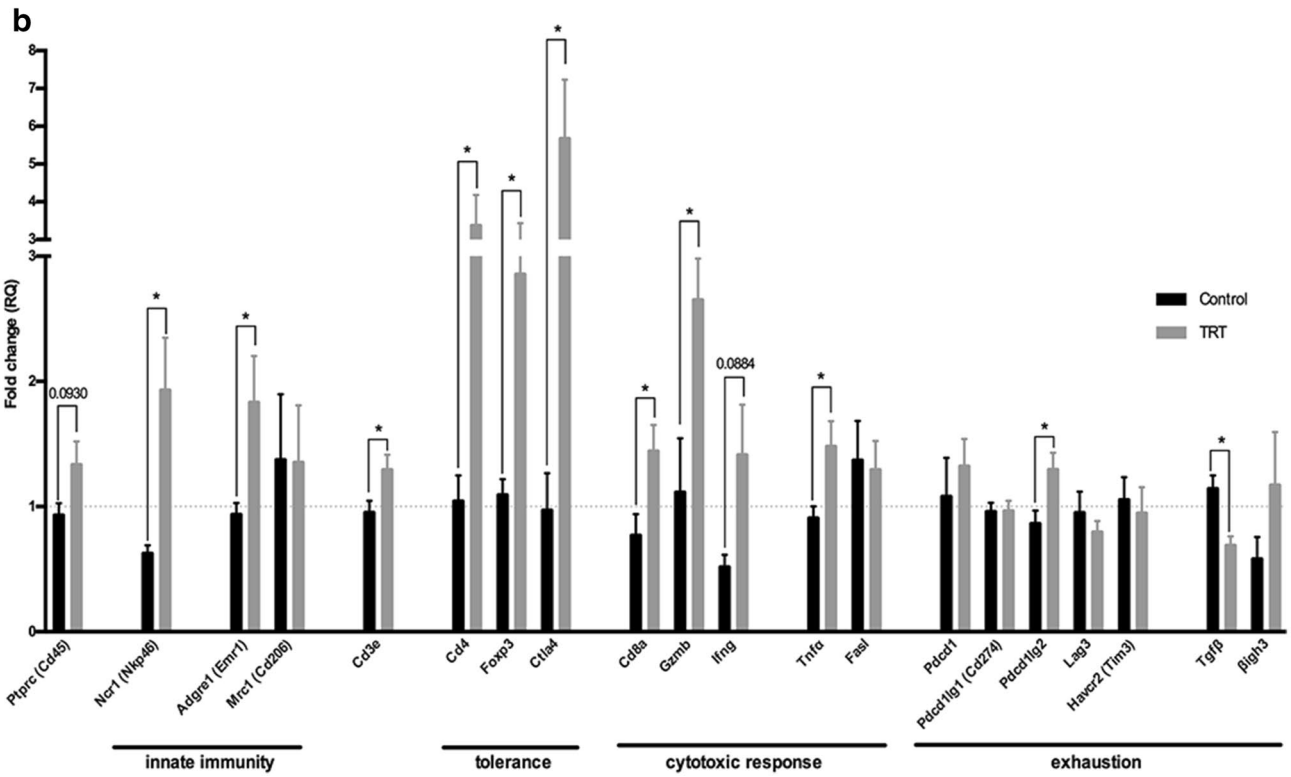
b
Fold change (RQ)
Control
TRT
0.0930
0.0884
Ptprc (Cd45)
Ncr1 (Nkp46)
Adgre1 (Emr1)
Mrc1 (Cd206)
Cd3e
Cd4
Foxp3
Ctla4
Cd8a
Gzmb
Ifng
Tnfa
Fasl
Pdcd1
Pdcd1lg1 (Cd274)
Pdcd1lg2
Lag3
Havcr2 (Tim3)
Tgfβ
βigh3
innate immunity
tolerance
cytotoxic response
exhaustion

◂**Fig. 2** TRT modifies tumor immune microenvironment. (**a**) Number of tumor infiltrating lymphocytes per gram was quantified by flow cytometry 3 days, 6 days and 12 days after irradiation ($n=6$ per time and condition). Gating was performed among $CD45^+$ cells. NK cells were identified as $CD3^-/NKp46^+$, CD8 T cells were identified as $CD3^+/CD8^+$ cells, CD4 T cells were identified as $CD3^+/CD4^+$ cells, and regulatory T cells were identified as $CD4^+/CD127^{low}$ cells. (**b**) Expression of immune response genes ten days after TRT assessed by RT-qPCR on two distant samples from each tumor (control: $n=4$, TRT: $n=5$)

and regulatory T cells was significantly increased: fourfold change for *Cd4* and *Foxp3* ($p=0.0260$ and $p=0.0123$, respectively) and sixfold change for *Ctla4* ($p=0.0385$). Exhaustion-related gene expression was not modified after TRT except *Pdcd1lg2*, which was significantly higher (1.5-fold change, $p=0.0325$).

These findings highlight the intratumoral recruitment of cytotoxic T cells, macrophages, NK cells and regulatory T cells after [$^{131}$I]ICF01012 injection. They also suggest that tolerogenic mechanisms prevail in the TRT-related immune response, whereas exhaustion seems less preponderant.

## [$^{131}$I]ICF01012 combined with immune checkpoint inhibitors

To assess further the role of exhaustion and tolerance in TRT-mediated immune response, we tested TRT combination with ICIs in B16F10 model. Survival and individual growth curves are shown in Fig. 3, and survival medians and tumor growth information are summarized in Table 1. Groups receiving the IgG isotype were not significantly different compared to control and TRT alone groups (Fig. 3b, Table 1).

### [$^{131}$I]ICF01012 induces tolerogenic immune mechanisms

To determine the importance of T cell exhaustion during TRT, we combined [$^{131}$I]ICF01012 with an anti-PD-1 antibody (Fig. 3c) or with an anti-PD-L1 antibody (Fig. 3d). Anti-PD1-groups showed a significant survival increase compared to TRT alone ($p<0.0001$) suggesting exhaustion mechanisms in non-treated tumors. However, TRT + anti-PD-1 survival was similar to the anti-PD-1 group (30 days). Interestingly, the group receiving TRT + anti-PDL-1 exhibited a small non-significant increase in survival compared to the anti-PD-L1 group (34 days vs 25 days, $p=0.104$). In TRT + ICI groups, tumor doubling times (DT) were not significantly different from the ICI alone groups (Table 1). These results suggest that $CD8^+$ T cell exhaustion is not preponderant in the TRT-mediated immune response.

RT-qPCR analyses suggested that tolerance is an important mechanism throughout TRT. We combined TRT with anti-CTLA-4 antibody (Fig. 3e). Interestingly, TRT + anti-CTLA-4 group showed a significant increase in survival compared to monotherapy groups (Fig. 3e, Table 2, 41 days vs. 27 days ($p=0.011$), vs. 26 days ($p<0.0001$), respectively). Doubling times in the TRT + anti-CTLA-4 group were also significantly higher compared to TRT alone and anti-CTLA-4 alone groups (Fig. 4c, 7.088 days$^{-1}$ vs 3.808 days$^{-1}$ vs 3.713 days$^{-1}$, respectively; $p<0.0001$). Additionally, combining TRT with anti-CTLA-4 extended the slow growth phase (26 days for TRT + anti-CTLA-4 vs. 19 days for anti-CTLA-4 alone). Furthermore, the interaction between TRT and anti-CTLA-4 was synergistic ($HR_{TRT+anti\text{-}CTLA\text{-}4}$ (0.08) < [$HR_{TRT}$ (0.626) x $HR_{anti\text{-}CTLA\text{-}4}$ (0.419)] = 0.262) [27], suggesting a major contribution of tolerance in the TRT-mediated immune response.

### TRT-induced tolerance reversal by anti-CTLA-4 Ab treatment favors T cell exhaustion

Induction of exhaustion occurs when anti-CTLA-4 is combined with external radiotherapy [10]. We hypothesized that the same phenomenon could occur during TRT. We added anti-PD-1 (Fig. 4a) or anti-PD-L1 (Fig. 4b) to the combination of TRT + anti-CTLA-4. On the one hand, the addition of anti-PD1 to the combination TRT + anti-CTLA-4 induced a 2.5 days gain of survival associated with a higher DT (Fig. 4c, 7.544 days$^{-1}$ vs 7.088 days$^{-1}$, ns). On the other hand, combining TRT + anti-CTLA-4 with anti-PD-L1 did not modify DT or median survival compared to TRT + anti-CTLA-4. However, the effects of this combination led to a more homogeneous response in terms of slow growth and DT compared to TRT + anti-CTLA-4. Interestingly, TRT + anti-CTLA-4 + anti-PD-L1 ($HR_{TRT+anti\text{-}CTLA\text{-}4+anti\text{-}PD\text{-}L1}$ (0.175) < [$HR_{TRT}$ (0.632) × $HR_{anti\text{-}CTLA\text{-}4+anti\text{-}PD\text{-}L1}$ (0.404)] = 0.255) was a synergistic combination, whereas TRT + anti-CTLA-4 + anti-PD-1 was only an additive association.

Using TLDA analyses (Fig. 4d), we compared TRT + anti-CTLA-4 gene expression with the gene expression of TRT + anti-CTLA-4 + anti-PD-1 group and TRT + anti-CTLA-4 + anti-PD-L1 group. TLDA analyses showed an increase in the exhaustion-related genes *Cd274*, *Lag3* and *Eomes* in the TRT + anti-CTLA-4 group compared to TRT + anti-CTLA-4 + anti-PD-1 ($p=0.0022$, $p=0.0079$ and $p=0.1438$, respectively) and to TRT + anti-CTLA-4 + anti-PD-L1 group ($p=0.0031$, $p=0.0670$ and $p=0.0396$, respectively). The addition of anti-PD-1 or anti-PD-L1 to TRT-CTLA4 combination induced a return to control values for

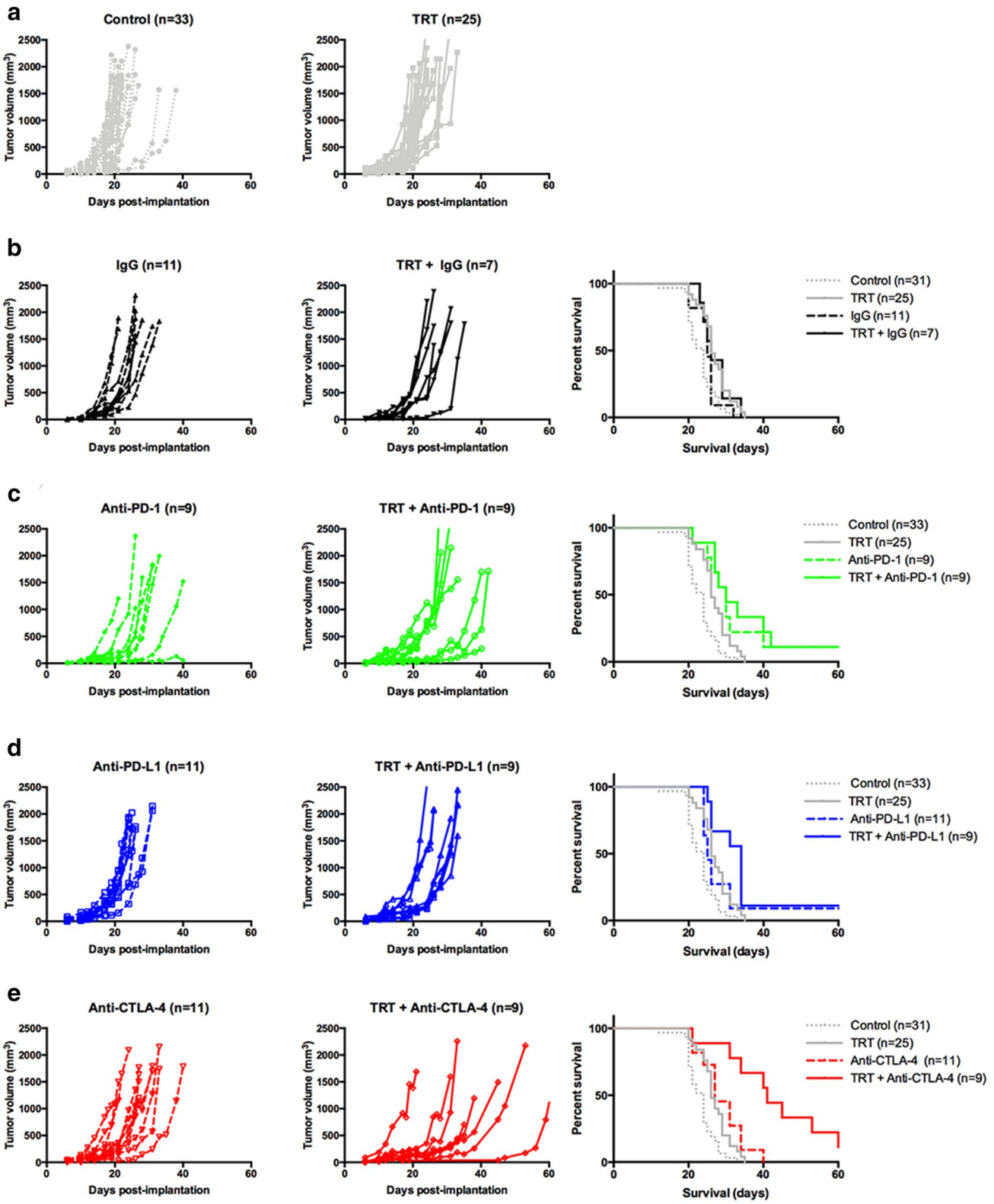


**Fig. 3** TRT combination with immune checkpoint inhibitors in monotherapy. Individual growth curves were represented for each pair of groups (control and TRT): (**a**) without immune checkpoint inhibitor, (**b**) isotype IgG, (**c**) anti-PD-1, (**d**) anti-PD-L1, (**e**) anti-CTLA-4. Kaplan–Meier survival curves were represented for each immune checkpoint inhibitor and compared with control and TRT group. Median survival and doubling times are resumed in Table 1

**Table 1** Survival and tumor growth characteristics for TRT + immune checkpoint inhibitor combination

| Group | Median survival (days) | *p* | Doubling times ($days^{-1}$) | *p* |
|---|---|---|---|---|
| Control ($n=33$) | 24.0 | 0.058 | 3.10 ± 0.14 | 0.2154 |
| TRT ($n=25$) | 26.0 | | 3.81 ± 0.17 | |
| IgG ($n=11$) | 25.0 | 0.379 | 2.85 ± 0.15 | > 0.9999 |
| TRT + IgG ($n=7$) | 26.0 | | 2.98 ± 0.20 | |
| Anti-PD-1 ($n=9$) | 30.0 | 0.693 | 3.34 ± 0.27 | 0.8414 |
| TRT + anti-PD-1 ($n=9$) | 30.0 | | 4.09 ± 0.32 | |
| Anti-PD-L1 ($n=11$) | 25.0 | 0.104 | 3.30 ± 0.21 | 0.5587 |
| TRT + anti-PD-L1 ($n=9$) | 34.0 | | 4.25 ± 0.43 | |
| Anti-CTLA-4 ($n=11$) | 27.0 | 0.011 | 3.71 ± 0.32 | < 0.0001 |
| TRT + anti-CTLA-4 ($n=9$) | 41.0 | | 7.09 ± 0.99 | |
| Anti-PD1 + anti-CTLA-4 ($n=10$) | 38.0 | 0.794 | 5.84 ± 0.60 | 0.0391 |
| TRT + anti-PD-1 + anti-CTLA-4 ($n=10$) | 43.5 | | 7.54 ± 0.64 | |
| Anti-PD-L1 + anti-CTLA-4 ($n=10$) | 29.5 | 0.091 | 4.74 ± 0.43 | 0.0003 |
| TRT + anti-PD-L1 + anti-CTLA-4 ($n=10$) | 36.0 | | 7.07 ± 0.66 | |

these three genes. All these results suggest that anti-CTLA-4 combined to TRT contributes to induce exhaustion.

### [$^{131}$I]ICF01012 combined with an original immunotherapy: TRT + anti-βig-h3

We have tested the effect of an anti-βig-h3mAb alone or combined with [$^{131}$I]ICF01012 in B16F10 model. Groups receiving the IgG isotype (Fig. 5b) did not show differences compared to the control and TRT alone groups (Fig. 5a). Anti-βig-h3 alone did not modify median survival compared to control group (Fig. 5c, 24 days). TRT + anti-βig-h3 group survival was significantly longer compared to anti-βig-h3 alone (29 days *vs* 24 days, $p=0.0297$). However, median survival in the combination TRT + anti-βig-h3 group did not reach statistical significance compared to other TRT groups. However, we showed a survival gain of 1.5 day (Supplementary Table 2). Additionally, we demonstrated a significant difference of tumor doubling times between the anti-βig-h3 group and TRT + anti-βig-h3 group ($p=0.0121$), with a difference between means of 0.94 ± 0.33 days (Fig. 5d).

## Discussion

This study allows a complete characterization of TRT-induced modifications in the antitumor immune response in the syngeneic B16F10 model. We demonstrate here that TRT using [$^{131}$I]ICF01012 induces immunogenic cell death which contributes to adaptive immune cell recruitment to the tumoral site. Thus, the efficacy of [$^{131}$I]ICF01012 on pigmented melanoma depends on the immune system and particularly on the adaptive immune response, as we established by comparing TRT effects between immunocompetent and immunodeficient mice. We also highlight that TRT modifies tumor immune microenvironment, especially by inducing cytotoxic T response and stimulating recruitment of innate immune cells as NK cells and macrophages. Similar to EBRT, escape mechanisms also occur throughout TRT. We demonstrate that tolerance, as well as regulatory T cell recruitment, is one of the main immune escape mechanisms in TRT. Additionally, the immunologic tolerance induced by TRT could be overcome by the use of an anti-CTLA-4 antibody at the cost of an induction of exhaustion, which could, however, be counteracted by the addition of an anti-PD-1 or anti-PD-L1 antibody. This hypothesis is supported by a previous study [10] on external radiation therapy by Twyman-Saint Victor et al.

Finally, we show that combining TRT and ICI is a promising approach for melanoma treatment. It indeed results without exception in a prolonged survival ($p<0.0001$) compared to [$^{131}$I]ICF01012 alone, especially in the case when ICI alone does not modify tumor growth (i.e., anti-CTLA-4, anti-PD-L1). Combining TRT + anti-CTLA-4 is the most promising combination with a significant increase in survival (15 days). Furthermore, approximately 22% of TRT + anti-CTLA-4-treated mice survived longer than 60 days, and one mouse turned out to be a very long responder (> 200 days). Interestingly, these results are quite similar to the observations [10] made by Twyman-Saint Victor et al. for the EBRT + anti-CTLA-4 combination in a B16F10 murine model. Contrasting with the

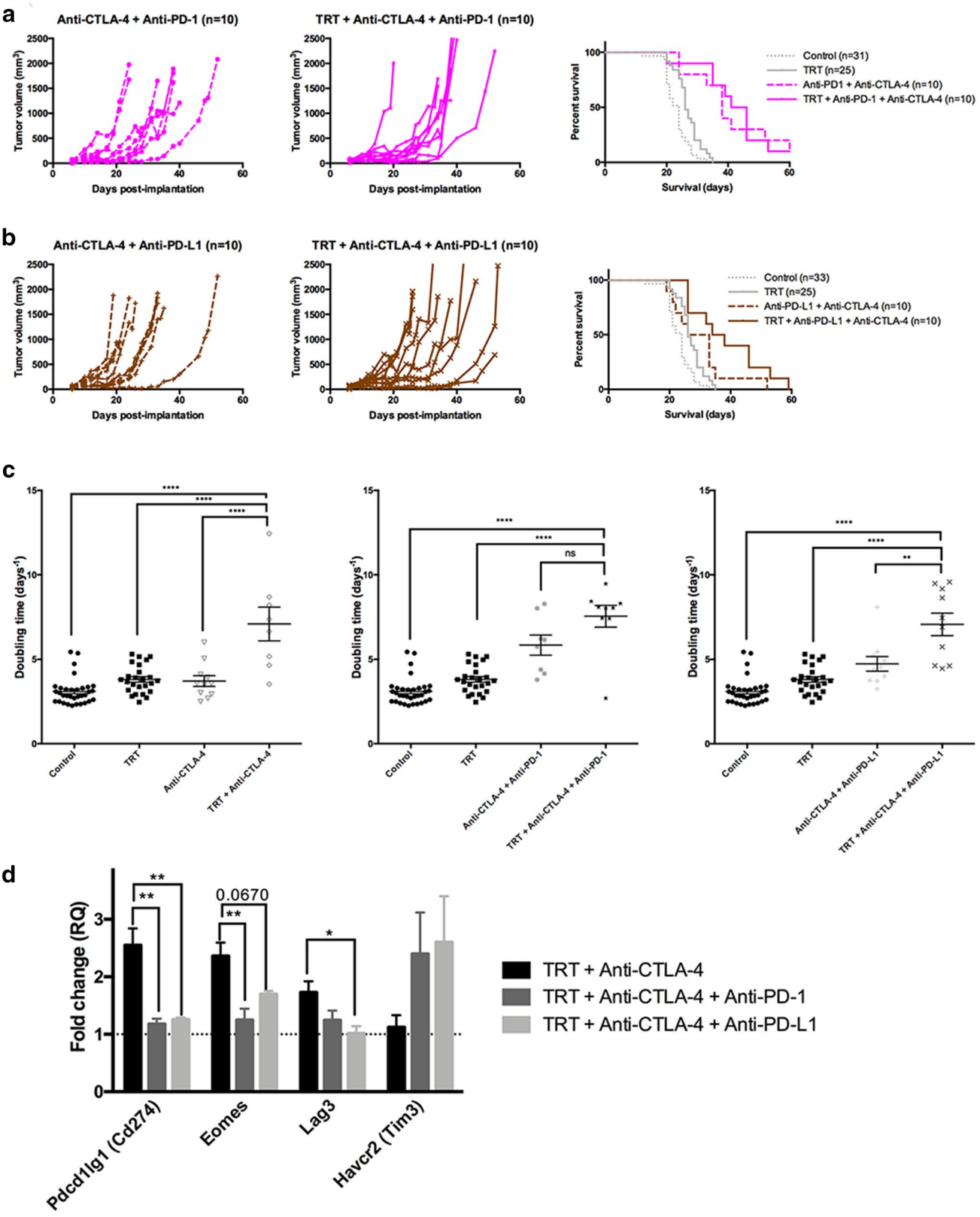
a
Anti-CTLA-4 + Anti-PD-1 (n=10)
TRT + Anti-CTLA-4 + Anti-PD-1 (n=10)
Tumor volume (mm3)
Days post-implantation
Percent survival
Survival (days)
Control (n=31)
TRT (n=25)
Anti-PD1 + Anti-CTLA-4 (n=10)
TRT + Anti-PD-1 + Anti-CTLA-4 (n=10)
b
Anti-CTLA-4 + Anti-PD-L1 (n=10)
TRT + Anti-CTLA-4 + Anti-PD-L1 (n=10)
Control (n=33)
TRT (n=25)
Anti-PD-L1 + Anti-CTLA-4 (n=10)
TRT + Anti-PD-L1 + Anti-CTLA-4 (n=10)
c
Doubling time (days-1)
Control
TRT
Anti-CTLA-4
TRT + Anti-CTLA-4
Anti-CTLA-4 + Anti-PD-1
TRT + Anti-CTLA-4 + Anti-PD-1
Anti-CTLA-4 + Anti-PD-L1
TRT + Anti-CTLA-4 + Anti-PD-L1
ns
d
Fold change (RQ)
0.0670
Pdcd1lg1 (Cd274)
Eomes
Lag3
Havcr2 (Tim3)
TRT + Anti-CTLA-4
TRT + Anti-CTLA-4 + Anti-PD-1
TRT + Anti-CTLA-4 + Anti-PD-L1

◂**Fig. 4** TRT combination with dual immune checkpoint inhibitors. Individual growth curves were represented for each pair of groups (control and TRT): (**a**) anti-PD-1 + anti-CTLA-4, (**b**) anti-PD-L1 + anti-CTLA-4. Kaplan–Meier survival curves were represented for each dual immune checkpoint inhibitor and compared with control and TRT group, (**c**) doubling times for anti-CTLA-4 groups, anti-PD-1 + anti-CTLA-4 groups and anti-PD-L1 + anti-CTLA-4 groups. (**d**) Exhaustion-related gene expression for anti-CTLA-4 groups, anti-PD-1 + anti-CTLA-4 groups and anti-PD-L1 + anti-CTLA-4 groups. Median survival and doubling times are resumed in Table 1.

results [19] reported by Choi et al., we observed a longer survival with either TRT alone, anti-CTLA-4 alone or ICI + TRT combination than what they described with dual ICI combined with TRT. This could be explained by three different factors: the fact that [$^{131}$I]ICF01012 does not target immune cells, the use of a lower dose (18.5 MBq vs 30 MBq) to limit hematotoxicity and the [$^{131}$I]ICF01012 pharmacokinetics (i.e., rapid clearance of non-target organs). We highlight also the safety of this type of combination without reporting any adverse events, especially no immune-related toxicity or melanin-related toxicity. Association of TRT with anti-βig-h3 shows an extend of survival that could probably be more detectable had we used a more immunogenic model such as B16-OVA [28, 29]. However, demonstrating efficiency of TRT + ICI combination in the less immunogenic murine B16F10 model is really promising for clinical use in human melanoma treatment since human melanoma has a higher mutational burden that leads to higher immunogenicity. These results validate the development of clinical trials for this type of combination. However, keeping in mind that murine and human melanoma have not the same immune behavior [28], anti-PD-1 should also be considered for combination as it is the most efficient ICI in human.

To conclude, we extend the knowledge on TRT-mediated immune response, demonstrating that tolerance is a prominent mechanism during [$^{131}$I]ICF01012 irradiation. [$^{131}$I]ICF01012 appears to be a good candidate in order to be used in combination with ICIs, with the advantages of a specific targeting and a high number of pigmented metastases treated at once. We eagerly expect the toxicity results of the phase 1 trial before proceeding with TRT + ICI combination therapy in a clinical trial.

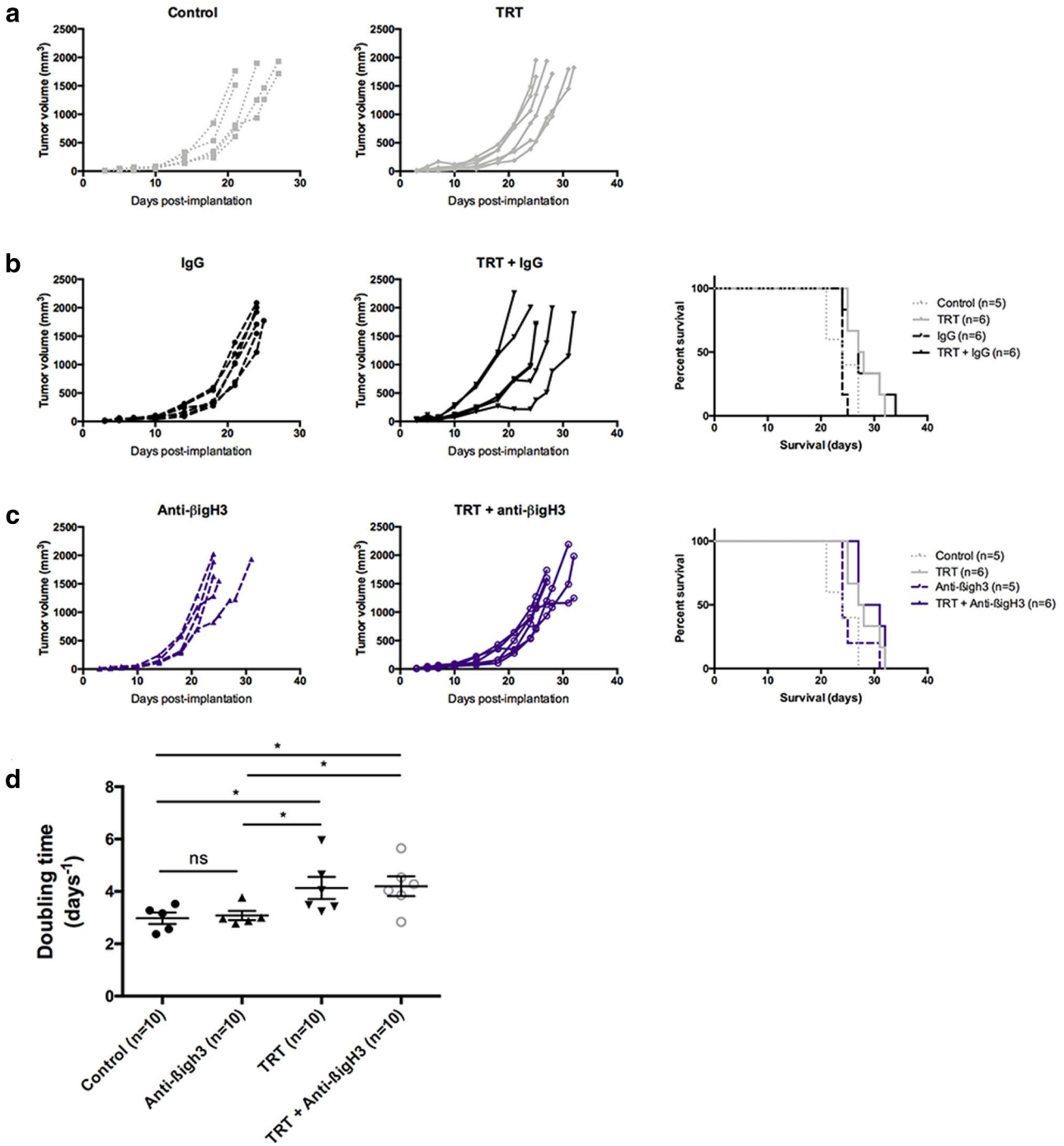


**Fig. 5** TRT combination with anti-βig-h3 antibody. Individual growth curves were represented for each pair of groups (control and TRT): (**a**) without immunotherapy, (**b**) isotype IgG, (**c**) anti-βig-h3. Kaplan–Meier survival curves were represented for each dual immune checkpoint inhibitor and compared with control and TRT group. (**d**) Doubling times for control, TRT, anti-βig-h3 alone and TRT + anti-βig-h3 groups. Median survival and doubling times are resumed in Table S2

**Acknowledgements** We are grateful to C.VACCHIAS from confocal imaging platform (CLIC) and to C.SOUBEYRAND-DAMON from histopathology platform (ANIPATH) for their pertinent advices. We thank M.GEMBARA for his kind proofreading of the English manuscript.

**Author contributions** JR, AH, SM, MD, FD and POR contributed to the study conception and design. Material preparation, data collection and analysis were performed by JR, VB, HA, SB, PA and SD. BP performed statistical analyses. The first draft of the manuscript was written by JR, and all authors commented on previous versions of the manuscript. All authors read and approved the final manuscript.

**Funding** This study was supported by the SFD – French Society for Dermatology and by the Ligue Régionale Contre le Cancer. J. ROUANET is supported by a doctoral fellowship granted by the SFD. H. AKIL was supported by a fellowship from the Auvergne Regional council and the European Community. A. Hennino is supported by INSERM TRANSFERT, Fondation Bristol-Meyers Squibb and La Ligue Régionale Contre le Cancer.

## Compliance with ethical standards

**Conflict of interest** The authors declare that they have no conflict of interest.

**Ethics approval** Experimentations on mice were in conformity with the Guide for the Care and Use of Laboratory Animals published by the US National Institutes of Health (8th edition, 2011) and were approved by local Ethic committee of Clermont-Ferrand (C2E2A No. 002) and French Ministry of Education and Research (Approval No. 12211). This article does not contain any studies with human participants performed by any of the authors.

## References

1. Lawrence MS, Stojanov P, Polak P, Kryukov GV, Cibulskis K, Sivachenko A, Carter SL, Stewart C, Mermel CH, Roberts SA, Kiezun A, Hammerman PS, McKenna A, Drier Y, Zou L, Ramos AH, Pugh TJ, Stransky N, Helman E, Kim J, Sougnez C, Ambrogio L, Nickerson E, Shefler E, Cortes ML, Auclair D, Saksena G, Voet D, Noble M, DiCara D, Lin P, Lichtenstein L, Heiman DI, Fennell T, Imielinski M, Hernandez B, Hodis E, Baca S, Dulak AM, Lohr J, Landau DA, Wu CJ, Melendez-Zajgla J, Hidalgo-Miranda A, Koren A, McCarroll SA, Mora J, Crompton B, Onofrio R, Parkin M, Winckler W, Ardlie K, Gabriel SB, Roberts CWM, Biegel JA, Stegmaier K, Bass AJ, Garraway LA, Meyerson M, Golub TR, Gordenin DA, Sunyaev S, Lander ES, Getz G (2013) Mutational heterogeneity in cancer and the search for new cancer-associated genes. Nature 499(7457):214–218. https://doi.org/10.1038/nature12213
2. Lee N, Zakka LR, Mihm MC Jr, Schatton T (2016) Tumour-infiltrating lymphocytes in melanoma prognosis and cancer immunotherapy. Pathology 48(2):177–187. https://doi.org/10.1016/j.pathol.2015.12.006
3. Portella L, Scala S (2019) Ionizing radiation effects on the tumor microenvironment. Semin Oncol. https://doi.org/10.1053/j.seminoncol.2019.07.003
4. Mason R, Au L, Ingles Garces A, Larkin J (2019) Current and emerging systemic therapies for cutaneous metastatic melanoma. Expert Opin Pharmacother 20(9):1135–1152. https://doi.org/10.1080/14656566.2019.1601700
5. Tai X, Van Laethem F, Pobezinsky L, Guinter T, Sharrow SO, Adams A, Granger L, Kruhlak M, Lindsten T, Thompson CB, Feigenbaum L, Singer A (2012) Basis of CTLA-4 function in regulatory and conventional CD4(+) T cells. Blood 119(22):5155–5163. https://doi.org/10.1182/blood-2011-11-388918
6. McDermott DF, Atkins MB (2013) PD-1 as a potential target in cancer therapy. Cancer Med 2(5):662–673. https://doi.org/10.1002/cam4.106
7. Lauden L, Siewiera J, Boukouaci W, Ramgolam K, Mourah S, Lebbe C, Charron D, Aoudjit F, Jabrane-Ferrat N, Al-Daccak R (2014) TGF-beta-induced (TGFBI) protein in melanoma: a signature of high metastatic potential. J Invest Dermatol 134(6):1675–1685. https://doi.org/10.1038/jid.2014.20
8. Goehrig D, Nigri J, Samain R, Wu Z, Cappello P, Gabiane G, Zhang X, Zhao Y, Kim IS, Chanal M, Curto R, Hervieu V, de La Fouchardiere C, Novelli F, Milani P, Tomasini R, Bousquet C, Bertolino P, Hennino A (2019) Stromal protein betaig-h3 reprogrammes tumour microenvironment in pancreatic cancer. Gut 68(4):693–707. https://doi.org/10.1136/gutjnl-2018-317570
9. Bauer CA (2019) Immunosuppressive betaig-h3 links tumour stroma and dysfunctional T cells in pancreatic cancer. Gut 68(4):581. https://doi.org/10.1136/gutjnl-2018-317735
10. Twyman-Saint Victor C, Rech AJ, Maity A, Rengan R, Pauken KE, Stelekati E, Benci JL, Xu B, Dada H, Odorizzi PM, Herati RS, Mansfield KD, Patsch D, Amaravadi RK, Schuchter LM, Ishwaran H, Mick R, Pryma DA, Xu X, Feldman MD, Gangadhar TC, Hahn SM, Wherry EJ, Vonderheide RH, Minn AJ (2015) Radiation and dual checkpoint blockade activate non-redundant immune mechanisms in cancer. Nature 520(7547):373–377. https://doi.org/10.1038/nature14292
11. Levy A, Massard C, Soria JC, Deutsch E (2016) Concurrent irradiation with the anti-programmed cell death ligand-1 immune checkpoint blocker durvalumab: Single centre subset analysis from a phase 1/2 trial. Eur J Cancer 68:156–162. https://doi.org/10.1016/j.ejca.2016.09.013
12. Roger A, Finet A, Boru B, Beauchet A, Mazeron JJ, Otzmeguine Y, Blom A, Longvert C, de Maleissye MF, Fort M, Funck-Brentano E, Saiag P (2018) Efficacy of combined hypo-fractionated radiotherapy and anti-PD-1 monotherapy in difficult-to-treat advanced melanoma patients. Oncoimmunology 7(7):e1442166. https://doi.org/10.1080/2162402X.2018.1442166
13. Pitt JM, Kroemer G, Zitvogel L (2017) Immunogenic and Non-immunogenic Cell Death in the Tumor Microenvironment. Adv Exp Med Biol 1036:65–79. https://doi.org/10.1007/978-3-319-67577-0_5
14. Baracco EE, Stoll G, Van Endert P, Zitvogel L, Vacchelli E, Kroemer G (2019) Contribution of annexin A1 to anticancer immunosurveillance. OncoImmunology. https://doi.org/10.1080/2162402X.2019.1647760
15. Wu Y, Pfeifer AK, Myschetzky R, Garbyal RS, Rasmussen P, Knigge U, Bzorek M, Kristensen MH, Kjaer A (2013) Induction of anti-tumor immune responses by peptide receptor radionuclide therapy with (177)Lu-DOTATATE in a murine model of a human neuroendocrine tumor. Diagnostics (Basel) 3(4):344–355. https://doi.org/10.3390/diagnostics3040344
16. Keisari Y, Hochman I, Confino H, Korenstein R, Kelson I (2014) Activation of local and systemic anti-tumor immune responses by ablation of solid tumors with intratumoral electrochemical or alpha radiation treatments. Cancer Immunol Immunother 63(1):1–9. https://doi.org/10.1007/s00262-013-1462-2
17. Chakraborty M, Gelbard A, Carrasquillo JA, Yu S, Mamede M, Paik CH, Camphausen K, Schlom J, Hodge JW (2008) Use of radiolabeled monoclonal antibody to enhance vaccine-mediated antitumor effects. Cancer Immunol Immunother 57(8):1173–1183. https://doi.org/10.1007/s00262-008-0449-x
18. Hernandez R, Walker KL, Grudzinski JJ, Aluicio-Sarduy E, Patel R, Zahm CD, Pinchuk AN, Massey CF, Bitton AN, Brown RJ, Sondel PM, Morris ZS, Engle JW, Capitini CM, Weichert JP (2019) (90)Y-NM600 targeted radionuclide therapy induces immunologic memory in syngeneic models of T-cell Non-Hodgkin's Lymphoma. Commun Biol 2:79. https://doi.org/10.1038/s42003-019-0327-4
19. Choi J, Beaino W, Fecek R, Fabian K, Laymon CM, Kurland B, Storkus W, Anderson CJ (2018) Combination treatment of VLA-4 targeted radionuclide therapy and immunotherapy in a mouse model of melanoma. J Nucl Med. https://doi.org/10.2967/jnumed.118.209510
20. Chezal JM, Papon J, Labarre P, Lartigue C, Galmier MJ, Decombat C, Chavignon O, Maublant J, Teulade JC, Madelmont JC,

Moins N (2008) Evaluation of radiolabeled (hetero)aromatic analogues of N-(2-diethylaminoethyl)-4-iodobenzamide for imaging and targeted radionuclide therapy of melanoma. J Med Chem 51(11):3133–3144. https://doi.org/10.1021/jm701424g

21. Bonnet M, Mishellany F, Papon J, Cayre A, Penault-Llorca F, Madelmont JC, Miot-Noirault E, Chezal JM, Moins N (2010) Anti-melanoma efficacy of internal radionuclide therapy in relation to melanin target distribution. Pigment Cell Melanoma Res 23(5):e1–11. https://doi.org/10.1111/j.1755-148X.2010.00716.x
22. Bonnet-Duquennoy M, Papon J, Mishellany F, Labarre P, Guerquin-Kern JL, Wu TD, Gardette M, Maublant J, Penault-Llorca F, Miot-Noirault E, Cayre A, Madelmont JC, Chezal JM, Moins N (2009) Targeted radionuclide therapy of melanoma: anti-tumoural efficacy studies of a new 131I labelled potential agent. Int J Cancer 125(3):708–716. https://doi.org/10.1002/ijc.24413
23. Viallard C, Perrot Y, Boudhraa Z, Jouberton E, Miot-Noirault E, Bonnet M, Besse S, Mishellany F, Cayre A, Maigne L, Rbah-Vidal L, D'Incan M, Cachin F, Chezal JM, Degoul F (2015) [(1)(2)(3)I]ICF01012 melanoma imaging and [(1)(3)(1)I]ICF01012 dosimetry allow adapted internal targeted radiotherapy in preclinical melanoma models. Eur J Dermatol 25(1):29–35. https://doi.org/10.1684/ejd.2014.2481
24. Degoul F, Borel M, Jacquemot N, Besse S, Communal Y, Mishellany F, Papon J, Penault-Llorca F, Donnarieix D, Doly M, Maigne L, Miot-Noirault E, Cayre A, Cluzel J, Moins N, Chezal JM, Bonnet M (2013) In vivo efficacy of melanoma internal radionuclide therapy with a 131I-labelled melanin-targeting heteroarylcarboxamide molecule. Int J Cancer 133(5):1042–1053. https://doi.org/10.1002/ijc.28103
25. Akil H, Rouanet J, Viallard C, Besse S, Auzeloux P, Chezal JM, Miot-Noirault E, Quintana M, Degoul F (2019) Targeted radionuclide therapy decreases melanoma lung invasion by modifying epithelial-mesenchymal transition-like mechanisms. Transl Oncol 12(11):1442–1452. https://doi.org/10.1016/j.tranon.2019.07.015
26. Viallard C, Chezal JM, Mishellany F, Ranchon-Cole I, Pereira B, Herbette A, Besse S, Boudhraa Z, Jacquemot N, Cayre A, Miot-Noirault E, Sun JS, Dutreix M, Degoul F (2016) Targeting DNA repair by coDbait enhances melanoma targeted radionuclide therapy. Oncotarget 7(11):12927–12936. https://doi.org/10.18632/oncotarget.7340
27. Raitanen M, Rantanen V, Kulmala J, Helenius H, Grenman R, Grenman S (2002) Supra-additive effect with concurrent paclitaxel and cisplatin in vulvar squamous cell carcinoma in vitro. Int J Cancer 100(2):238–243. https://doi.org/10.1002/ijc.10472
28. Yu JW, Bhattacharya S, Yanamandra N, Kilian D, Shi H, Yadavilli S, Katlinskaya Y, Kaczynski H, Conner M, Benson W, Hahn A, Seestaller-Wehr L, Bi M, Vitali NJ, Tsvetkov L, Halsey W, Hughes A, Traini C, Zhou H, Jing J, Lee T, Figueroa DJ, Brett S, Hopson CB, Smothers JF, Hoos A, Srinivasan R (2018) Tumor-immune profiling of murine syngeneic tumor models as a framework to guide mechanistic studies and predict therapy response in distinct tumor microenvironments. PLoS ONE 13(11):e0206223. https://doi.org/10.1371/journal.pone.0206223
29. Schaue D, Ratikan JA, Iwamoto KS, McBride WH (2012) Maximizing tumor immunity with fractionated radiation. Int J Radiat Oncol Biol Phys 83(4):1306–1310. https://doi.org/10.1016/j.ijrobp.2011.09.049